Organic & Biomolecular Chemistry

Accepted Manuscript

This article can be cited before page numbers have been issued, to do this please use: H. Matsumoto, Y. Nishimura and T. Arai, *Org. Biomol. Chem.*, 2017, DOI: 10.1039/C7OB01376K.

ROYAL SOCIETY OF CHEMISTRY

rsc.li/obc

View Article Online
DOI: 10.1039/C7OB01376K

Organic & Biomolecular Chemistry

PAPER

Excited State Intermolecular Proton Transfer Dependent on Substitution Pattern of Anthracene–Diurea Compounds involved in Fluorescent ON[1]–OFF–ON[2] response by the Addition of Acetate Ions

Received 00th January 20xx,
Accepted 00th January 20xx

DOI: 10.1039/x0xx00000x

www.rsc.org/

Hisato Matsumoto, Yoshinobu Nishimura, and Arai Tatsuo*

We report anthracene–diurea compounds allows us an anion sensor by using the fluorescence emission control depending on the substitution position on the anthracene ring. Anthracene–diurea compounds exhibit different excited-state intermolecular proton transfer (ESIPT) reactions depending on the pattern of the substituents. Three new anthracene–diurea compounds, which have two phenylurea groups substituted at different positions on anthracene, were synthesized. These compounds formed a complex with acetate ions through intermolecular hydrogen bonding between N–H and C=O moieties in the ground state. It was revealed that the difference in the position of the substituents greatly impacted the excited state intermolecular proton transfer. Whereas **1,5BPUA** having the urea group at 1 and 5 positions exhibited ESIPT reaction, which is energetically favourable to form its tautomer, in the presence of TBAAc, **2,6BPUA** having the urea group at low electron density positions, 2 and 6 positions, showed no ESIPT reaction due to the inversion of the LUMO energy levels of normal and tautomer states. As a result of detailed spectroscopic measurements, we found that the LUMO energy level of the normal form was lowered due to the urea group acting as an electron-withdrawing group. In addition, we revealed that **9,10BPUA** had strong electronic interactions between the two phenylurea moieties at 9 and 10 positions, and caused an ON[1]–OFF–ON[2] response for acetate ions. Our findings offer molecular design guidelines for the material having an anthracene moiety dependent on the substitution pattern of anthracene derivatives.

Introduction

Proton transfer reactions are one of the most basic reactions and are functionally important in numerous biological, chemical and physical processes.[1-6] Excited state intermolecular proton transfer (ESIPT) reactions are used in various applications in pH,[7] photolithography,[8] proton transfer lasers,[9,10] organic electro-luminescence materials,[11] and probes of the environment around proteins,[12-14] micelles[15-17] and cyclodextrin.[18-21] An ESIPT reaction requires a molecule with a proton donor group and one with a proton accepting group that form intermolecular hydrogen bonds in the ground state. Upon exciting the hydrogen bonds, the acid−base properties of the proton donor and the proton accepting groups reverse, causing the excited normal form (N*) to be at a higher energy than the conjugate excited tautomer (T*).

Graduate School of Pure and Applied Sciences, University of Tsukuba, 1-1-1 Tennoudai, Tsukuba, Ibaraki 305-8571, Japan. E-mail: arai@chem.tsukuba.ac.jp; Fax: +81-29-853-6503; Tel: +81-29-853-4315

† Electronic supplementary information (ESI) available. See DOI: 10.1039/x0xx00000x

A typical proton donor group is urea. Its N–H group has a δ^+ character and can form a hydrogen bond with a chemical species having a δ^- character. Thus, much research has been

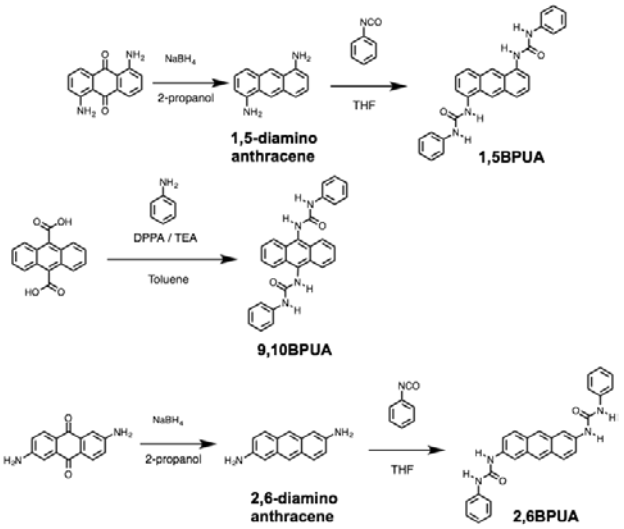

Scheme 1. Synthetic routes of **1,5BPUA**, **9,10BPUA** and **2,6BPUA**.

devoted to anion sensors utilizing intermolecular hydrogen bonding interactions between urea and anion species.[22,23]

In our previous research, we studied the photochemistry of urea derivatives containing aromatic fluorophore molecules and their hydrogen-bonding interactions with anion species.[24-29] In particular, 1-anthracen-*n*-yl-3-phenylurea (*n***PUA**; *n* = 1, 2 and 9) in the presence of tetrabutylammonium acetate (TBAAc) formed a complex through intermolecular hydrogen bonding between N–H and C=O moieties in the ground state, followed by an ESIPT reaction. These studies revealed the influence of the substitution pattern of anthracene for ESIPT by introducing phenylurea groups at positions 1, 2 and 9 of anthracene. In fact, we found that the rate constant of ESIPT (k_{PT}) depended significantly on the position of the phenylurea substituents. The k_{PT} of **1PUA**, with a phenylurea group introduced at the 1-position of anthracene, is 2.4×10^9 s^{-1}, while the k_{PT} of **2PUA** is 5×10^7 s^{-1}, i.e., the k_{PT} of **1PUA** is 50 times larger than that of **2PUA**. Other experiments show that the photodimerization, luminescence and electrochemical properties depend on the position of the anthracene substituents.[25,28,30-35] However, research on the ESIPT of anthracene–urea compounds has been limited.

Many compounds having two or more anion recognition sites have been reported as anion sensors. The fluoride ion sensor, in which two phenylurea groups are immobilized on the 1,8-position of anthracene, recognizes one anion by using two urea groups.[36] Chemosensors, designed as "receptor-spacer-fluorophore-spacer-receptor" conjugates, recognize dicarboxylates and pyrophosphate by photoinduced electron transfer quenching of the anthracene moiety.[37] Recently, we reported an anthracene–diurea compound having two phenylurea groups on the 9,10-position of anthracene. This compound exhibited unique emission. While the fluorescence of the urea compound (ON^1) was quenched in the presence of a low concentration of acetate ions (OFF), fluorescence enhancement occurred upon addition of a high concentration of acetate ions (ON^2). Thus, we succeeded in developing an ON^1–OFF–ON^2 sensor for acetate ions, depending on their concentration.[29] As described above, different anion recognition mechanisms can be realized by the manipulation of the substitution.[38]

In this study, we synthesized anthracene–diurea compounds, **1,5BPUA**, **9,10BPUA** and **2,6BPUA**, in which two phenylurea groups are immobilized on the 1,5-, 9,10- and 2,6-positions of anthracene, respectively (Scheme 1). These compounds were examined spectroscopically for changes in fluorescence properties upon addition of TBAAc. Among these compounds, only **1,5BPUA** caused ESIPT in the presence of TBAAc, whereas all anthracene–monophenylurea compounds (*n***PUA**) caused ESIPT. In **9,10BPUA**, it was revealed that the two phenylurea moieties showed electronic interactions with each other, and this interaction was closely related to for ON^1–OFF–ON^2 response. Furthermore, to explore the ESIPT reaction and ON^1–OFF–ON^2 response by changing the substitution pattern of the two phenylurea groups, we used kinetic analysis and calculation of free energy in the excited state. As a result of these studies, we found that it is possible to regulate the ESIPT reaction and the ON^1–OFF–ON^2 response by changing the substitution pattern of the two phenylurea groups.

Experimental

Methods

^{1}H NMR spectra were recorded on a Bruker ARX-400 (400 MHz for ^{1}H) spectrometer using DMSO-d_6 as a solvent and tetramethylsilane as an internal standard. Absorption and fluorescence spectra were measured on Shimadzu UV-1600 and Hitachi F–4500 fluorescence spectrometers, respectively. Fluorescence decay measurements were performed using a time-correlated single-photon counting method. Laser excitation at 375 nm was performed using a diode laser (PicoQuant, LDH-P-C-375) with a power control unit (PicoQuant, PDL 800-B), with a repetition rate of 2.5 MHz. The temporal profiles of the fluorescence decays were detected by a microchannel plate photomultiplier (Hamamatsu, R3809U) equipped with a TCSPC computer board module (Becker and Hickl, SPC630). The full width at half maximum (fwhm) of the instrument response function was 51 ps.[39] The values of χ^2 and the Durbin–Watson parameters were used to determine the quality of the fit obtained by nonlinear regression.[40] DMSO (spectroscopic grade, Wako Pure Chemical Industries, Japan) was used as a solvent without further purification. Acetate ions were in the form of TBAAc, which contains a tetrabutylammonium cation (Sigma-Aldrich, Japan). All measurements were carried out at room temperature under an Ar atmosphere. The concentrations were adjusted so that the absorption maximum of the excitation wavelength was about 0.1 for each sample. Density functional theory (DFT) calculations were performed using the Spartan '04 program (Wavefunction, Inc., Irvine, CA, USA).

Synthesis

All solvents and 1,5-diaminoanthraquinone, 2,6-diaminoanthraquinone, phenyl isocyanate, aniline, diphenylphosphoryl azide, triethylamine and 9,10-anthracenedicarboxylic acid were purchased from Wako Pure Chemical Industries, Ltd., Japan, Tokyo Chemical Industry Co., Ltd., Japan, or Aldrich, USA and were used without further purification.

1,5-Diaminoanthracene: To a 100-mL two-necked round bottom flask were added 1,5-diaminoanthraquinone (940 mg, 3.94 mmol), $NaBH_4$ (4.4 g, 0.12 mol) and 2-propanol (20 mL). After stirring for 14 h at 80 °C, the solvent was removed by suction filtration. The residue was washed by MeOH to give a black solid (713 mg, 87%). ^{1}H NMR (DMSO-d_6, 270 MHz): δ 5.28 (s, 4H), 5.38 (d, J = 4.0 Hz, 2H), 6.62 (d, J = 5.0 Hz, 2H), 6.88 (d, J = 5.0 Hz, 2H), 7.05 (t, J = 5.0 Hz, 2H)

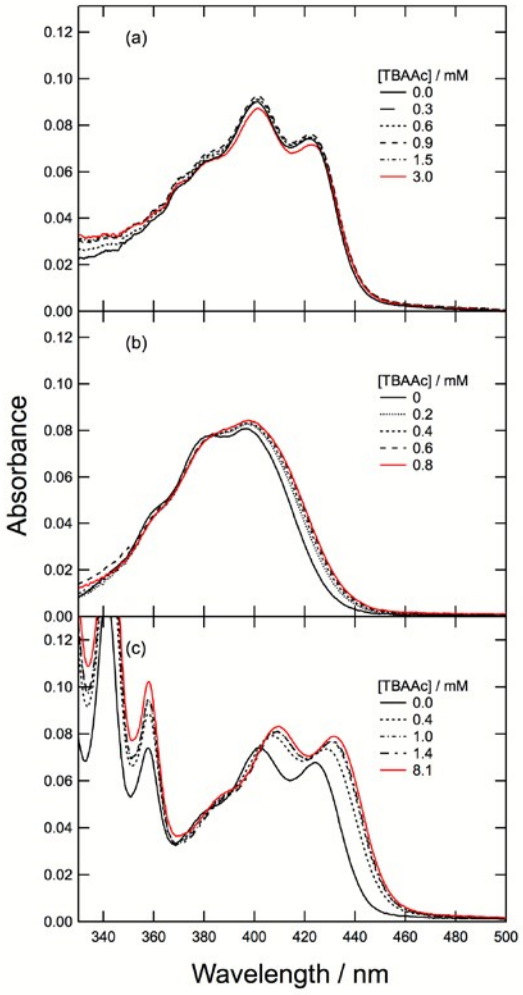

Fig 1. Changes in the absorption spectra of (a) **1,5BPUA** (9.8×10^{-6} M), (b) **9,10BPUA** (8.6×10^{-6} M), (c) **2,6BPUA** (1.1×10^{-5} M) in the presence of TBAAc.

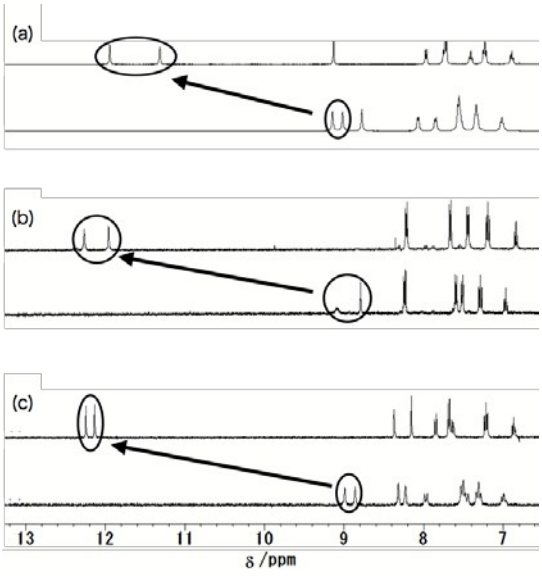

Fig 2. ^{1}H NMR spectra of (a) **1,5BPUA**, (b) **9,10BPUA**, (c) **2,6BPUA** in the presence (top) and absence (bottom) of TBAAc in DMSO-d_6.

1,5BPUA: To a 100-mL two-necked round bottom flask were added 1,5-diaminoanthracene (150 mg, 0.72 mmol), phenyl isocyanate (40 µL, 0.33 mmol) and dry THF (20 mL). After stirring for 70 h at 70 °C, the solvent was removed by suction filtration. The residue was washed by MeOH to give a black solid (89 mg, 28%). ^{1}H NMR (DMSO-d_6, 270 MHz): δ 7.02 (t, J = 7.8 Hz, 2H), 7.34 (dd, J = 8.3 Hz, J = 6.9 Hz, 4H), 7.41-7.50 (m, 6H), 7.85 (dd, J = 8.4 Hz, J = 6.7 Hz, 2H), 8.07 (d, J = 6.9 Hz, 2H), 8.78 (s, 2H), 9.02 (s, 2H), 9.15 (s, 2H). HRMS *m/z* (ESI-MS) calcd for $C_{28}H_{22}N_4NaO_2^+$ ([M + Na]$^+$), 469.1635; found, 469.1630.

9,10BPUA: To a two-necked round bottom flask (100 mL) were added 9,10-anthracenedicarboxylic acid (206 mg, 0.773 mmol), toluene (80 mL), triethylamine (210 µL, 1.51 mmol), and diphenylphosphoryl azide (150 µL, 1.85 mmol). After stirring for 30 min at 80 °C, aniline (150 mg, 1.64 mmol) in toluene (5 mL) was added, and the mixture was refluxed for 91 h. The solvent was filtered by suction filtration and the residue was washed with methanol a number of times to give a light yellow solid (43.5 mg, 12%). ^{1}H NMR (DMSO-d_6, 400 MHz): δ 6.97 (t, J = 7.4 Hz, 2H), 7.29 (t, J = 7.4 Hz, 4H), 7.51 (t, J = 7.4 Hz, 4H), 7.58-7.61 (m, 4H), 8.23-8.26 (m, 4H), 8.79 (s, 2H), 9.08 (s, 2H). HRMS *m/z* (ESI-MS) calcd for $C_{28}H_{22}N_4NaO_2^+$ ([M + Na]$^+$), 469.1635; found, 469.1645.

2,6-Diaminoanthracene: To a 100-mL two-necked round bottom flask were added 2,6-diaminoanthraquinone (1100 mg, 4.61 mmol), $NaBH_4$ (4.2 g, 0.11 mol) and 2-propanol (40 mL). After stirring for 12 h at 80 °C, the solvent was removed by suction filtration. The residue was washed with MeOH to give a light yellow solid (866 mg, 90%). ^{1}H NMR (DMSO-d6, 270 MHz): δ 5.15 (s, 4H), 6.71 (s, 2H), 6.85 (d, J = 7.0 Hz, 2H), 7.55 (d, J = 7.0 Hz, 2H), 7.74 (s, 2H).

2,6BPUA: To a 100-mL two-necked round bottom flask were added 2,6-diaminoanthracene (153 mg, 0.73 mmol), phenyl isocyanate (190 µL, 1.59 mmol) and dry THF (55 mL). After stirring for 24 h at 70 °C, the solvent was removed by suction filtration. The residue was washed by MeOH to give a light yellow solid (40 mg, 12%). ^{1}H NMR (DMSO-d_6, 270 MHz): δ 6.99 (t, J = 6.8 Hz, 2H), 7.31 (t, J = 6.8 Hz, 4H), 7.43-7.52 (m, 6H), 7.97 (d, J = 9.7, 2H), 8.23 (s, 2H), 8.32 (s, 2H), 8.86 (s, 2H), 8.99 (s, 2H). HRMS *m/z* (ESI-MS) calcd for $C_{28}H_{22}N_4NaO_2^+$ ([M + Na]$^+$), 469.1635; found, 469.1638.

Measurement of ^{13}C NMR spectra was unsuccessful due to the low solubilities of **1,5BPUA**, **9,10BPUA** and **2,6BPUA**.

Results

Absorption spectra

Figure 1 shows the absorption spectra of **1,5BPUA**, **9,10BPUA** and **2,6BPUA** in DMSO with various concentrations of TBAAc. In the absence of TBAAc, the spectral shape for **1,5BPUA** was broad compared to that of the parent molecule, anthracene, which had vibrational structure (Fig. 1a). The wavelength maxima were 400 and 421 nm, with shoulders at 381 and 368 nm. There was a slight increase in the absorption band in the presence of TBAAc. The spectral shape

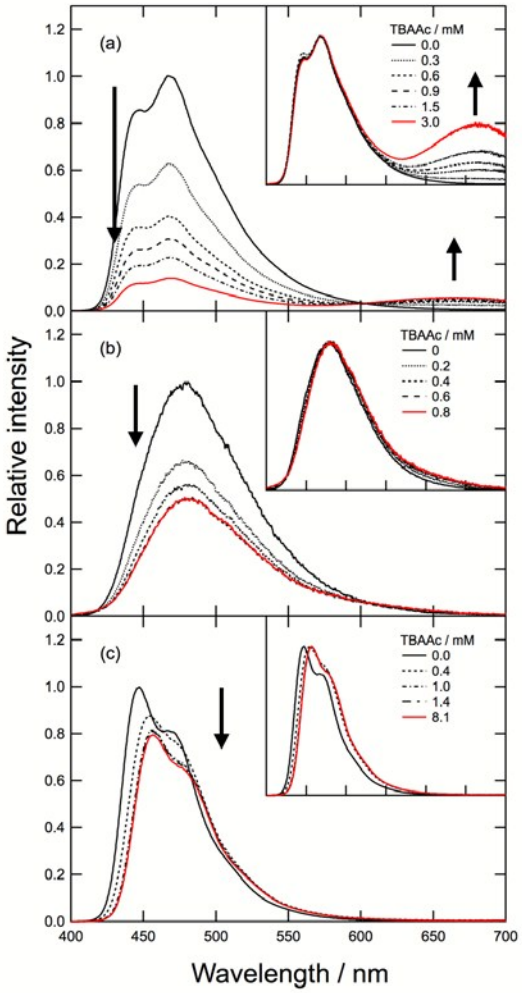

Fig 3. Changes in the fluorescence spectra of (a) **1,5BPUA** (9.8×10^{-6} M), (b) **9,10BPUA** (8.6×10^{-6} M), (c) **2,6BPUA** (1.1×10^{-5} M) in the presence of TBAAc. The insets show normalized spectra at maximum intensity.

for **9,10BPUA** was broader than that for **1,5BPUA** (Fig. 1b). The wavelength maxima for **9,10BPUA** were 381 and 396 nm with shoulders at 359 and 342 nm. The red-edge absorption band longer than 383 nm was red-shifted in the presence of TBAAc. In contrast, the spectral shape for **2,6BPUA** was completely different from those for **1,5BPUA** and **9,10BPUA**, with strong vibrational bands from 320 to 420 nm, as shown in Fig. 1c. The red-edge absorption band (greater than 404 nm) was red-shifted in the presence of TBAAc, while the absorbance below 300 nm increased significantly.

^{1}H NMR spectra

To confirm the complexation of **1,5BPUA**, **9,10BPUA** and **2,6BPUA** with TBAAc, ^{1}H NMR spectra were measured in the absence and presence of TBAAc (Fig. 2). This revealed hydrogen-bonding interactions between **1,5BPUA** and TBAAc, since downfield shifts of the N–H protons from 9.15 and 9.01 ppm to 11.94 and 11.32 ppm, respectively, were observed in the presence of TBAAc (Fig. 2a). The signals for **9,10BPUA** also exhibited downfield shifts from 9.08 and 8.79 ppm to 12.26 and 11.96 ppm, respectively (Fig. 2b). Similarly, the signals for **2,6BPUA** exhibited downfield shifts from 8.99 and 8.86 ppm to 12.24 and 12.14 ppm, respectively (Fig. 2c). These shifts indicate that **BPUA**s interact with TBAAc through hydrogen bonding.

Association constants

The association constants for **1,5BPUA**, **9,10BPUA** and **2,6BPUA** with TBAAc were determined according to eq. 1 to be 1.9×10^3, 5.3×10^3 and 5.2×10^3 M^{-1}, respectively,[41]

$$\frac{1}{I-I_0} = \frac{1}{I_{max}-I_0}\left(\frac{1}{K_a[A]} + 1\right) \quad (1)$$

where I_0 and I are the fluorescence intensities for the host monitored at the wavelength of the fluorescence maximum in the absence and presence of anions, respectively, [A] is the total anion concentration, and I_{max} is the fluorescence intensity for **BPUA**s fully hydrogen bonded with the anion (Fig. S6 in the ESI). However, since **1,5BPUA** and **2,6BPUA** showed only a one-step change in the absorption and fluorescence spectra, we calculated only K_{a1} (association constant of 1:1 complex). **9,10BPUA** showed a two-step change in the fluorescence spectra (ON^1–OFF–ON^2), therefore K_{a1} and K_{a2} (association constants for 1:1 complex and 1:2 complex, respectively) could be calculated by the fluorescence change (K_{a2} = 270 M^{-1}).[29] The difference in the association constants for **BPUA**s may arise from the acidity of the urea protons. The association constants for **1,5BPUA** and **2,6BPUA** were similar to those for **1PUA** and **2PUA**, respectively, while that for **9,10BPUA** was 3.3 times larger than that for **9PUA**.[25,26]

Fluorescence spectra

Figure 3a shows changes in the fluorescence spectra of **1,5BPUA** in the presence of various concentrations of TBAAc in DMSO. While the spectrum in the absence of TBAAc had a maximum at 468 nm with a shoulder at 447 nm, the fluorescence intensity decreased as the TBAAc concentration increased from 0 to 3.0 mM followed by the appearance of a new band with a maximum at 665 nm as shown in the inset of Fig. 3a. The peak wavelength for **1,5BPUA** remained unchanged even in the presence of 3.0 mM TBAAc. The fluorescence changes in **9,10BPUA** were very characteristic (Fig. 3b). While the spectrum in the absence of TBAAc had a maximum at 480 nm, the fluorescence intensity decreased with increasing concentration of TBAAc from 0 to 0.8 mM followed by the appearance of a weak new band in the long-wavelength region. As shown in Fig. S7 in the ESI, when the TBAAc concentration was increased further to 91.8 mM, the intensity of the band at 483 nm increased. This indicated that while the fluorescence of **9,10BPUA** in DMSO (ON^1) was quenched in the presence of low concentration of acetate anion due to suppressing ESIPT reaction (OFF), fluorescence enhancement occurred by the addition of high concentration of acetate anion due to suppressing ESIPT (ON^2)[29]. The fluorescence intensity for **2,6BPUA** showed a smaller decrease than that for **1,5BPUA** in the presence of 0.6 mM TBAAc (Fig. 3b). For **2,6BPUA**, an increase in the TBAAc concentration resulted in a decrease in fluorescence intensity and a red-shift of the spectrum

View Article Online
DOI: 10.1039/C7OB01376K

Table 1. Lifetimes of **1,5BPUA**, **9,10BPUA** and **2,6BPUA** in the absence and presence of TBAAc

1,5BPUA			**9,10BPUA**			**2,6BPUA**		
	τ / ns			τ / ns			τ / ns	
[TBAAc]/mM	450 nm	630 nm	[TBAAc]/mM	450 nm	600 nm	[TBAAc]/mM	450 nm	600 nm
0	6.89 (1.00)	–	0	3.39 (1.00)	–	0	16.5 (1.00)	–
	6.78 (0.44)	5.40 (1.00)		3.65 (0.77)	1.67 (0.41)		15.2 (0.97)	21.0 (0.33)
0.3	0.83 (0.56)	0.54 (–1.00)	0.8	1.40 (0.23)	3.49 (0.59)	1.0	3.03 (0.03)	11.3 (0.58)
					2.49 (–1.00)			1.21 (0.09)

The values in parentheses are the normalized amplitudes for the respective lifetimes.

without a new emission band around 600-700 nm. The new band of **1,5BPUA** had a maximum at 665 nm and may be the tautomer emission, which is generated by the ESIPT reaction.[24] In contrast, **2,6BPUA** showed no tautomer emission due to the lack of an ESIPT reaction and **9,10BPUA** emitted only a slight tautomeric fluorescence in the presence of 0.8 mM TBAAc. This indicates that the complexes of these two compounds with TBAAc caused almost no ESIPT reaction, and/or the fluorescence quantum yield of the tautomer was very low. The fact that only **1,5BPUA** caused an ESIPT reaction in **BPUA**s by the addition of TBAAc is in contrast to all anthracene–monourea compounds (*n***PUA**) that cause an ESIPT reaction.[24,25]

Lifetimes of BPUAs in the excited state

The fluorescence decay of **1,5BPUA** in the absence of TBAAc under Ar gave a monoexponential curve with a lifetime of 6.89 ns (Table 1, see Figs. S8–S13 in the ESI). The fluorescence curve observed at 440 nm in the presence of 3.0 mM TBAAc exhibited a biexponential decay with lifetimes of 6.78 and 0.83 ns, while the curve at 630 nm showed rise and decay times of 0.54 and 5.40 ns, respectively. The fluorescence decay for **9,10BPUA** in the absence of TBAAc under Ar exhibited a monoexponential curve with a lifetime of 3.39 ns. The fluorescence curve observed at 450 nm in the presence of 1.0 mM TBAAc exhibited a biexponential decay with lifetimes of 3.65 and 1.40 ns, and the curve at 650 nm showed a biexponential decay with lifetimes of 3.49 and 1.67 ns and rise of 2.49 ns. The fluorescence decay for **2,6BPUA** in the absence of TBAAc under Ar gave a single exponential curve with a lifetime of 16.5 ns. However, the fluorescence curve observed at 440 nm in the presence of 10 mM TBAAc showed biexponential decay with lifetimes of 15.2 and 3.03 ns, while the curve at 630 nm showed a tri-exponential decay with lifetimes of 21.0, 11.3 and 1.21 ns. The time development of the new emission was confirmed by time-resolved spectra of **1,5BPUA** (see Fig. S14 in the ESI). The build-up of new emission spectra maximized around 650 and 520 nm was confirmed at 5.3 and 7.2 ns for **1,5BPUA** and **9,10BPUA**, whereas no new emission spectra at longer wavelengths in the time-resolved spectrum of **2,6BPUA** appeared (see Figs. S14–S16 in the ESI).

Discussion

Difference in the fluorescence properties of BPUAs

To investigate the substitution effects of urea moieties on the photochemical behavior, we focused on the changes in the fluorescence properties and the reactivity of intermolecular proton transfer. Differences in the interactions between urea groups were observed in the fluorescence spectra in the presence of TBAAc. **1,5BPUA** showed no spectral shift and a monotonic decrease in emission with increasing TBAAc concentration. To examine the emissive properties of the complex of **BPUA**s with TBAAc in more detail, we investigated the relationship between the proportion of free **BPUA**, which is uncomplexed **BPUA** with TBAAc, and the fluorescence intensity. The proportion of free **BPUA** can be calculated by equations (2)-(4),

$$[\mathbf{BPUA}\cdots \mathrm{AcO}^-] = \frac{\alpha - \sqrt{\alpha^2 - 4[\mathrm{TBAAc}][\mathbf{BPUA}]_0}}{2} \quad (2)$$

$$\alpha = [\mathrm{TBAAc}] + [\mathbf{BPUA}]_0 + {}^1/_{K_a} \quad (3)$$

$$\frac{[\text{free } \mathbf{BPUA}]}{[\mathbf{BPUA}]_0} = \frac{[\mathbf{BPUA}]_0 - [\mathbf{BPUA}\cdots \mathrm{AcO}^-]}{[\mathbf{BPUA}]_0} \quad (4)$$

where [**BPUA**···AcO⁻], [TBAAc], [**BPUA**]$_0$ and [free **BPUA**] are the concentrations of the complex of **BPUA** with TBAAc, the total TBAAc, the initial **BPUA**, and the **BPUA** uncomplexed with TBAAc, respectively. In the presence of 3.0 mM TBAAc, the proportion of free **1,5BPUA** is about 15%, which is consistent with the relative fluorescence intensity for free **1,5BPUA** (see Fig. S17 in the ESI). This indicates that the complex of **1,5BPUA** with TBAAc may have almost no emissive properties. In contrast, the fluorescence spectra of the complex of **2,6BPUA** with TBAAc exhibited different behavior. Although the proportion of free **2,6BPUA** was less than 1% in the presence of 30.5 mM TBAAc, the relative fluorescence intensity for **2,6BPUA** was 0.57 times that in the absence of TBAAc (see Fig. S18 in the ESI). Furthermore, the fluorescence spectrum of **2,6BPUA** under the addition of TBAAc showed an emissive red-shifted band relative to that for free **2,6BPUA**. This indicates that unlike **1,5BPUA**, the complex of **2,6BPUA** with TBAAc is luminescent. We can

surmise an associative form by the fluorescence lifetimes.[27,28] A complicated associative state may exist due to two phenylurea moieties of **2,6BPUA**. We inferred that the associative form between **2,6BPUA** and TBAAc consists of multiple luminescent lifetimes, which suggests that there are multiple complexes such as **2,6BPUA**···AcO⁻ and **2,6BPUA**···2AcO⁻. By contrast, the sum of the proportion of free **9,10BPUA** and **9,10BPUA**···2AcO⁻ is roughly agreement with the relative fluorescence intensity. This indicates that free **9,10BPUA** and **9,10BPUA**···2AcO⁻ are luminescent while **9,10BPUA**···AcO⁻ is non-luminescent (see Fig. S19 in the ESI).

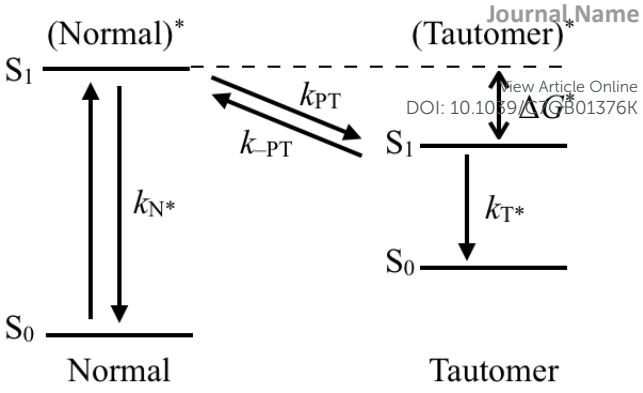

Scheme 2. Reaction scheme for ESIPT.

Kinetic analysis of excited state intermolecular proton transfer reactions

As described above, the fluorescence properties of **BPUA**s in the presence of TBAAc depend on the position of urea substituents on the anthracene ring. In particular, it is noteworthy that only **1,5BPUA** gave an ESIPT reaction in the presence of TBAAc, whereas **2,6BPUA** and **9,10BPUA** showed no remarkable tautomer emission. These differences in the fluorescence properties of **BPUA**s may arise from the electronic interactions between urea groups depending on the substitution pattern of the anthracene ring. To examine the interaction between urea groups, we compared the relevant spectra and rate constants for **BPUA**s with those for ***n*PUA**, which has only one phenylurea moiety.

According to the reaction scheme shown in Scheme 2, the differential rate equations for the change in concentration of **BPUA**···AcO⁻ (normal, N*) and the tautomer (T*) in the excited state can be expressed as follows:[25,42-49]

$$\frac{d[\mathrm{N}^*]}{dt} = -(k_{\mathrm{N}^*} + k_{\mathrm{PT}}) \times [\mathrm{N}^*] + k_{-\mathrm{PT}} \times [\mathrm{T}^*] \quad (5)$$

$$\frac{d[\mathrm{T}^*]}{dt} = -(k_{\mathrm{T}^*} + k_{-\mathrm{PT}}) \times [\mathrm{T}^*] + k_{\mathrm{PT}} \times [\mathrm{N}^*] \quad (6)$$

where k_{PT} and $k_{-\mathrm{PT}}$ denote the forward and reverse ESIPT rate constants, respectively, and k_{N^*} and k_{T^*} are the decay rate constants for the excited normal and tautomer forms, respectively. The integration of equations (5) and (6) with the given initial conditions at t = 0, $[\mathrm{N}^*] = [\mathrm{N}^*]_0$ and $[\mathrm{T}^*] = [\mathrm{T}^*]_0$ = 0 gives equations (7) and (8) for $[\mathrm{N}^*]$ and $[\mathrm{T}^*]$:

$$[\mathrm{N}^*] = \frac{[\mathrm{N}^*]_0}{\gamma_1 - \gamma_2} \times [(X - \gamma_2)exp(-\gamma_1 t) - (X - \gamma_1)exp(-\gamma_2 t)] \quad (7)$$

$$[\mathrm{T}^*] = \frac{k_{\mathrm{PT}}[\mathrm{N}^*]_0}{\gamma_1 - \gamma_2} \times [exp(-\gamma_2 t) - exp(-\gamma_1 t)] \quad (8)$$

where

$$\gamma_1 = \frac{1}{2}\left[(X+Y) + \sqrt{(X-Y)^2 + 4k_{\mathrm{PT}}k_{-\mathrm{PT}}}\right] \quad (9)$$

$$\gamma_2 = \frac{1}{2}\left[(X+Y) - \sqrt{(X-Y)^2 + 4k_{\mathrm{PT}}k_{-\mathrm{PT}}}\right] \quad (10)$$

$$X = k_{\mathrm{N}^*} + k_{\mathrm{PT}}, \quad Y = k_{\mathrm{T}^*} + k_{-\mathrm{PT}} \quad (11)$$

$$\gamma_1 + \gamma_2 = X + Y = k_{\mathrm{N}^*} + k_{\mathrm{T}^*} + k_{\mathrm{PT}} + k_{-\mathrm{PT}} \quad (12)$$

An iterative fitting method was applied to the deconvoluted decay curve to determine the four unknown rate constants, which are correlated with eq. (12), in the presence of TBAAc, according to a previously reported calculation method.[50]

The k_{N^*}, k_{T^*}, k_{PT} and $k_{-\mathrm{PT}}$ values were calculated to be 1.6×10^8, 3.5×10^8, 5.3×10^8, and 2.5×10^8 s^{-1}, respectively, for **1,5BPUA** and 2.2×10^8, 3.9×10^8, 1.6×10^8, and 2.3×10^8 s^{-1} for **9,10BPUA**. The Gibbs free energy change, ΔG^*, as shown in Scheme 2, and equilibrium constant (K_{eq}) for the complex and the tautomer in the excited state at 298 K were estimated as follows: [26,48]

$$\Delta G^* = -RTlnK_{\mathrm{eq}}, \quad K_{eq} = \frac{k_{PT}}{k_{-PT}} \quad (13)$$

The K_{eq} and ΔG^* values were calculated to be 2.1 and –1.9 kJ/mol, respectively, for **1,5BPUA** and 0.70 and 0.90 kJ/mol for **9,10BPUA**. The ΔG^* value for **2,6BPUA** might be slightly greater than that for **9,10BPUA** since no tautomer of **2,6BPUA** was observed in the presence of TBAAc. An exergonic ESIPT reaction involving **1,5BPUA**···AcO⁻ is responsible for the dual fluorescence consisting of free **1,5BPUA** and the tautomer. In contrast, the endergonic ESIPT reaction involving **9,10BPUA**···AcO⁻ may explain the much weaker tautomer emission due to the small amount of T* generation.[48,51,52]

The differences between the energy levels of the normal and tautomer forms play an important role in the relevant rate constants for an ESIPT reaction. To calculate the 0–0 transition energy for the normal form ($E_{0\text{–}0}$), the intersection of absorption and fluorescence spectra was used. The $E_{0\text{–}0}$ energies for **1,5BPUA**, **9,10BPUA** and **2,6BPUA** in the presence of TBAAc are 275.0, 273.1 and 270.0 kJ/mol, respectively, while those for **1PUA**, **9PUA** and **2PUA** are 281.0, 289.7 and 279.5 kJ/mol, respectively. The introduction of two urea groups results in a decrease in the $E_{0\text{–}0}$ energy, which is associated with the LUMO energy level.[53,54] Since the phenylurea moiety acts as an electron-withdrawing group, the $E_{0\text{–}0}$ energies of **BPUA**s might be affected by the stabilization of the LUMO energy resulting from the introduction of two phenylurea groups.

To examine $E_{0\text{–}0}$ in a different way, it is worthwhile to determine the spectral shape for the tautomer to estimate its energy levels. The emission spectral shape for the tautomer

form except for **2,6BPUA** was derived by simply subtracting the emission spectrum of **1,5BPUA** and **9,10BPUA** in the absence of TBAAc from that in the presence of TBAAc. The resulting peak wavelengths for **1,5BPUA** and **9,10BPUA** were estimated to be 660 and 615 nm, respectively (see Fig. S20, S21 in the ESI), which correspond to the energy gap between the ground and excited states for the tautomer. As described above, the substitution effect on the energy level may appear to be more significant stabilization of the excited state than the ground state.[53,54] By calculating the energy for the tautomer based on its fluorescence wavelength, the emissive state of the tautomer of **1,5BPUA** was found to be stabilized by 13.28 kJ/mol relative to that for **9,10BPUA**, which is consistent with the contribution of more extended π-conjugation in **1,5BPUA** than in the tautomer of **9,10BPUA**. The reason why the tautomer of **1,5BPUA** is stabilized compared with those of **2,6BPUA** and **9,10BPUA** is unknown due to the yet-to-be-defined structure of the tautomer. However, we revealed that stabilization of the tautomer of **1,5BPUA** might cause a significant excited-state energy gap between the normal and tautomer forms leading to the negative Gibbs free energy change involved in the tautomer generation.

These differences in fluorescence properties of **BPUA**s may be related to differences in the electronic state of **BPUA**s originated by the substitution position of an anthracene ring, which may affects to the electronic interaction between the two phenylurea moieties.[29] The vibrational structure of the absorption spectrum of **2,6BPUA** was more remarkable than those of **1,5BPUA** and **9,10BPUA**. Differences in vibration structure of the absorption spectra imply that the electronic interaction between the anthracene and urea moieties of **2,6BPUA** is weaker than those of **9,10BPUA** and **1,5BPUA** due to low electron density positions, 2 and 6 positions[25]. Therefore, since the electronic coupling of **2,6BPUA** between the anthracene and urea moieties is weaker than those of **1,5BPUA** and **9,10BPUA**, the charge delocalization of **2,6BPUA** followed by ESIPT reaction reduces relative those of **1,5BPUA** and **9,10BPUA**. Consequently, the substitution position dependence of the electronic coupling for charge delocalization might affect ΔG^* although the details remain unknown.

Since the decay rate constants for the tautomer (k_{T*}) are the sum of the radiative and nonradiative rate constants, they relate to the amount of T^* produced. The fluorescence intensities for T^* depend on the product of the amount of T^* generated multiplied by the fluorescence quantum yield of T^*. Although the tautomer of **1,5BPUA** was clearly seen, that of **9,10BPUA** could barely be observed by fluorescence. This may be explained by the small amount of T^* generated and the relatively low fluorescence quantum yield for T^*.

The origin of the ON^1–OFF–ON^2 reaction in 9,10BPUA

To investigate the mechanism of the ON^1–OFF–ON^2 reaction in **9,10BPUA**, differences in the electronic interactions depending on the substitution position were examined. It is well-known that the electron density for anthracene increases sequentially in the order of 2 < 1 < 9 positions.[55] Therefore, it is expected that the electronic interaction of the anthracene–ring with the urea group also increase in the same order. The vibrational structures in the absorption spectra of **1,5BPUA** and **2,6BPUA** were quite similar to those for **1PUA** and **2PUA**, respectively, whereas that for **9,10BPUA** is broader than that for **9PUA**.[24] Differences in the vibrational structure of the absorption spectra indicate that the electronic interaction between the anthracene and urea moieties of **9,10BPUA** is greater than that for **2,6BPUA** and **1,5BPUA**. The maximum wavelengths in the fluorescence spectra of **1,5BPUA** and **2,6BPUA** were similar to those for **1PUA** and **2PUA** (see Fig. S22, S23 in the ESI), while those for **9,10BPUA** and **9PUA** were distinctly different from each other (see Fig. S24 in the ESI). The introduction of a phenylurea moiety resulted in a red shift of the fluorescence peak of **9,10BPUA** up to 480 nm, compared with that of **9PUA** (450 nm). This indicates that the phenylurea moiety acts as an electron-withdrawing group, thereby significantly reducing the LUMO energy level.

Differences in the electronic interaction between the anthracene and urea moieties affect the fluorescence properties and association constants in the presence of TBAAc.[25] This electron–withdrawing effect can also be considered to affect the difference in the association constants for TBAAc. The association constant for **9,10BPUA** was 5300 M^{-1}, which is 3.3 times larger than that for **9PUA** (1600 M^{-1}). In general, the strength of hydrogen bonding depends on the acidity of the hydrogen donor. This implies that one phenylurea moiety may act as an electron-withdrawing group against the other phenylurea group, such that the electron density in the nitrogen atom of the urea moiety bound with an acetate ion is lower in **9,10BPUA** than in **9PUA**. However, the association constants for **1,5BPUA** and **2,6BPUA** were similar to those for **1PUA** and **2PUA**, respectively, indicating that the phenylurea moieties of **1,5BPUA** and **2,6BPUA** have less electron-withdrawing ability than that for **9,10BPUA**. These results suggest that **9,10BPUA** has strong interactions between the two phenylurea moieties, whereas **1,5BPUA** and **2,6BPUA** have negligibly weak interactions. The difference in this interaction is closely related to the ON^1–OFF–ON^2 response observed in **9,10BPUA** for acetate ions. The urea moiety hydrogen-bonded with TBAAc may behave as an electron-donating group while the phenylurea group without TBAAc acts as an electron-withdrawing group. The resonance effect of the two electron-donating urea groups that interact with each other may cause the ON^1–OFF–ON^2 response.[29] Thus, **9,10BPUA**, which has a strong interaction between phenylurea moieties, induces an ON^1–OFF–ON^2 response, while **1,5BPUA** and **2,6BPUA**, which have weak interactions between phenylurea moieties, cause only an ON–OFF response.

Conclusions

We found that anthracene–diurea compounds (**1,5BPUA**, **9,10BPUA** and **2,6BPUA**) exhibited a significant difference in the ESIPT reaction due to their ΔG^*, which depends on the positions of the two urea moieties substituted on the anthracene

ring, i.e., only **1,5BPUA** underwent the ESIPT reaction in the presence of TBAAc through the form of **1,5BPUA**···AcO^-. Furthermore, from a kinetic analysis of the ESIPT reaction, we revealed that the substitution position affects both the energy levels of the LUMO and the rate constants associated with ESIPT. In addition, we found that the ON^1–OFF–ON^2 response of **9,10BPUA** for acetate ions arises from a specific charge density of the 9,10-positions in the anthracene ring, which is involved in π-conjugation with the anthracene ring. This study might provide new knowledge for the molecular design of fluorescent materials using a substitution position effect of anthracene rings.

Conflicts of interest

There are no conflicts of interest to declare.

Notes and references

1 B. G. Malmstrom, *Chem. Rev.* 1990, **90**, 1247-1260.
2 *Electron and Proton Transfer in Chemistry and Biology*, ed. A. Muller, H. Ratajczak, W. Junge and E. Diemann, Elsevier, Amsterdam, 1992, Vol. 78.
3 L. G. Arnaut and S. J. Formosinho, *J. Photochem. Photobiol. A-Chem.* 1993, **75**, 1-20.
4 P. Jaramillo, K. Coutinho and S. Canuto, *J. Phys. Chem. A* 2009, **113**, 12485-12495.
5 B. K. Paul and N. Guchhait, *J. Phys. Chem. B* 2010, **114**, 12528-12540.
6 G. Cui, Z. Lan and W. Thiel, *J. Am. Chem. Soc.* 2012, **134**, 1662-1672.
7 J. H. Clark, S. L. Shapiro, A. J. Campillo and K. R. Winn, *J. Am. Chem. Soc.* 1979, **101**, 746-748.
8 E. S. Mansueto and C. A. Wight, *J. Am. Chem. Soc.* 1989, **111**, 1900-1901.
9 P. Chou, D. McMorrow, T. J. Aartsma and M. Kasha, *J. Phys. Chem.* 1984, **88**, 4596-4599.
10 A. U. Acuna, A. Costela and J. M. Munoz, *J. Phys. Chem.* 1986, **90**, 2807-2808.
11 S. Park, J. E. Kwon, S. H. Kim, J. Seo, K. Chung, S.-Y. Park, D.-J. Jang, B. M. Medina, J. Gierschner and S. Y. Park, *J. Am. Chem. Soc.* 2009, **131**, 14043-14049.
12 M. R. Loken, L. Brand, J. W. Hayes and J. R. Gohlke, *Biochemistry* 1972, **11**, 4779-4786.
13 S. K. Mondal, S. Ghosh, K. Sahu, P. Sen and K. Bhattacharyya, *J. Chem. Sci.* 2007, **119**, 71-76.
14 F. A. S. Chipem, S. K. Behera and G. Krishnamoorthy, *Photochem. Photobiol. Sci.* 2014, **13**, 1297-1304.
15 M. J. Politi and H. Chaimovich, *J. Phys. Chem.* 1986, **90**, 282-287.
16 A. Phukon, N. Barman and K. Sahu, *Langmuir* 2015, **31**, 12587-12596.
17 A. Phukon, S. Ray and K. Sahu, *Langmuir* 2016, **32**, 6656-6665.
18 N. Chattopadhyay, *J. Photochem. Photobiol. A-Chem.* 1991, **58**, 31-36.
19 J. L. Prados, A. G. Leon, A. I. Olives, M. A. Martin and B. Del Castillo, *J. Photochem. Photobiol. A-Chem.* 2005, **173**, 287-295.
20 M. Mukhopadhyay, D. Banerjee and S. Mukherjee, *J. Phys. Chem. A* 2006, **110**, 12743-12751.
21 F. A. S. Chipem, S. K. Behera and G. Krishnamoorthy, *J. Phys. Chem. A* 2013, **117**, 4084-4095.
22 V. Amendola, L. Fabbrizzi and L. Mosca, *Chem. Soc. Rev.* 2010, **39**, 3889-3915.
23 V. B. Bregovic, N. Basaric and K. Mlinaric-Majerski., *Coord. Chem. Rev.* 2015, **295**, 80-124.
24 I. Ohshiro, M. Ikegami, Y. Shinohara, Y. Nishimura and T. Arai, *Bull. Chem. Soc. Jpn.* 2007, **80**, 747-751.
25 S. Ikedu, Y. Nishimura and T. Arai, *J. Phys. Chem. A* 2011, **115**, 8227-8233.
26 H. Masai, S. Ikedu, Y. Nishimura and T. Arai, *J. Photochem. Photobiol. A-Chem.* 2012, **250**, 1-5.
27 H. Matsumoto, Y. Nishimura and T. Arai, *Bull. Chem. Soc. Jpn*. 2015, **88**, 1100-1104.
28 H. Matsumoto, Y. Nishimura and T. Arai, *Photochem. Photobiol. Sci.* 2016, **15**, 1071-1079.
29 H. Matsumoto, Y. Nishimura and T. Arai, *Photochem. Photobiol.* DOI: 10.1111/php.12768
30 Y. Mizobe, N. Tohnai, M. Miyata and Y. Hasegawa, *Chem. Commun.* 2005, 1839-1841.
31 Y. Mizobe, H. Ito, I. Hisaki, M. Miyata, Y. Hasegawa and N. Tohnai, *Chem. Commun.* 2006, 2126-2128.
32 H. Kudo, M. Yamamoto, T. Nishikubo and O. Moriya, *Macromolecules* 2006, **39**, 1759-1765.
33 J. R. Quinn, F. W. Foss, Jr., L. Venkataraman, M. S. Hybertsen and R. Breslow, *J. Am. Chem. Soc.* 2007, **129**, 6714.
34 J. R. Quinn, F. W. Foss, Jr., L. Venkataraman and R. Breslow, *J. Am. Chem. Soc.* 2007, **129**, 12376.
35 J. Kim, Y. Oka, T. Morozumi, E. W. Choi and H. Nakamura, *Tetrahedron* 2011, **67**, 4814-4819.
36 J. Y. Kwon, Y. J. Jang, S. K. Kim, K. H. Lee, J. S. Kim and J. Y. Yoon, *J. Org. Chem.* 2004, **69**, 5155-5157.
37 T. Gunnlaugsson, A. P. Davis, J. E. O'rien and M. Glynn, *Org. Lett.* 2002, **4**, 2449-2452.
38 P. Buhlmann, S. Nishizawa, K. P. Xiao and Y. Umezawa, *Tetrahedron* 1997, **53**, 1647-1654.
39 Y. Nishimura, M. Kamada, M. Ikegami, R. Nagahata and T. Arai, *J. Photochem. Photobiol. A-Chem.* 2006, **178**, 150-155.
40 N. Boens, N. Tamai, I. Yamazaki and T. Yamazaki, *Photochem. Photobiol.* 1990, **52**, 911-917.
41 S. Feryforgues, M. T. Lebris, J. P. Guette and B. Valeur, *J. Phys. Chem.* 1988, **92**, 6233-6237.
42 T. Okada, T. Saito, N. Mataga, Y. Sakata and S. Misumi, *Bull. Chem. Soc. Jpn.* 1977, **50**, 331-336.
43 M. Migita, T. Okada, N. Mataga, Y. Sakata, S. Misumi, N. Nakashima and K. Yoshihara, *Bull. Chem. Soc. Jpn.* 1981, **54**, 3304-3311.
44 T. Okada, M. Migita, N. Mataga, Y. Sakata and S. Misumi, *J. Am. Chem. Soc.* 1981, **103**, 4715-4720.
45 J. N. Demas. *Excited State Lifetime Measurements*, Academic Press, New York, 1983, pp. 59-62.
46 V. V. Shynkar, Y. Mely, G. Duportail, E. Piemont, A. S. Klymchenko and A. P. Demchenko, *J. Phys. Chem. A* 2003, **107**, 9522-9529.
47 P. T. Chou, W. S. Yu, Y. M. Cheng, S. C. Pu, Y. C. Yu, Y. C. Lin, C. H. Huang and C. T. Chen, *J. Phys. Chem. A* 2004, **108**, 6487-6498.
48 K.-C. Tang, M.-J. Chang, T.-Y. Lin, H.-A. Pan, T.-C. Fang, K.-Y. Chen, W.-Y. Hung, Y.-H. Hsu and P.-T. Chou, *J. Am. Chem. Soc.* 2011, **133**, 17738-17745.
49 S. Tasaki, A. Momotake, Y. Kanna, T. Sato, Y. Nishimura and T. Arai, *Photochem. Photobiol. Sci.* 2015, **14**, 1864-1871.
50 Y. Nishimura, K. Shimamura, Y. Ohmori, Y. Shinohara and T. Arai, *J. Photochem. Photobiol. A-Chem.* 2011, **218**, 69-75.
51 H.-W. Tseng, J.-Q. Liu, Y.-A. Chen, C.-M. Chao, K.-M. Liu, C.-L. Chen, T.-C. Lin, C.-H. Hung, Y.-L. Chou, T. Lin, T.-L.

View Article Online
DOI: 10.1039/C7OB01376K

Wang and P.-T. Chou, *J. Phys. Chem. Lett.* 2015, **6**, 1477-1486.
52 C. Azarias, S. Budzak, A. D. Laurent, G. Ulrich and D. Jacquemin, *Chem. Sci.* 2016, **7**, 3763-3774.
53 J. L. Bredas and A. J. Heeger, *Chem. Phys. Lett.* 1994, **217**, 507-512.
54 H. Zhou, L. Yang, A. C. Stuart, S. C. Price, S. Liu and W. You, *Angew. Chem. Int. Ed.* 2011, **50**, 2995-2998.
55 I. A. Fedorov, Y. N. Zhuravlev and V. P. Berveno, *Phys. Chem. Chem. Phys.* 2011, **13**, 5679-5686.

View Article Online
DOI: 10.1039/C7OB01376K

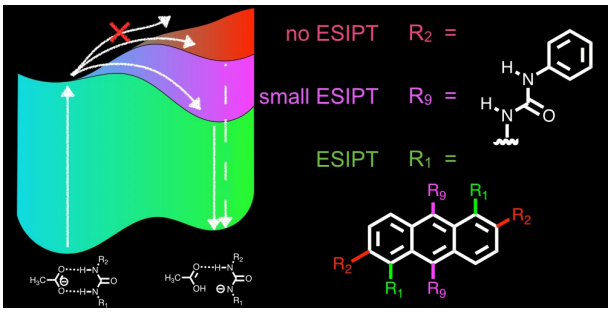

Anthracene–diurea compounds exhibit different excited-state intermolecular proton transfer (ESIPT) reactions depending on the pattern of the substituents.